

## Supporting Information

### Langmuir-Blodgett Films of Salophen-based Metallosurfactants as Surface Pretreatment Coatings for Corrosion Mitigation

Sunalee Gonawala,<sup>†</sup> Verônica R. Leopoldino,<sup>†,§</sup> Kenneth Kpogo,<sup>†</sup> and Cláudio N. Verani<sup>†,\*</sup>

<sup>†</sup> Department of Chemistry, Wayne State University, Detroit, MI 48202, USA

<sup>§</sup> Department of Chemical Engineering, Universidade Federal de São João del Rei,  
Ouro Branco, MG 36420, Brazil

#### Contents:

**1. Experimental Section.**

*a. Materials and methods.*

**2. Synthesis and characterizations.**

*a. Synthesis of  $[Zn^{II}(L^{N2O2})H_2O]$  (**2**).*

**3. Mass Spectrum for Complex 2.**

*a. Figure S1. Experimental (bars) and simulated (line) isotopic distribution for the molecular ions of  $[Zn^{II}(L^{N2O2}) + H^+]^+$ .*

**4. X-ray structural determination for  $[Zn^{II}(L^{N2O2})H_2O/MeOH]$  (**2**).**

*a. Table S1. Selected X-ray crystal data for complex 2.*

**5. Electronic Spectrum for Complex 2.**

*a. Figure S2. UV-visible spectrum of **2** in  $1 \times 10^{-5}$  M dichloromethane.*

**6. Electrochemical Data for the Complex 2.**

*a. Figure S3. Cyclic voltammogram of **2** in dichloromethane. Conditions: 0.1 M TBAPF<sub>6</sub> as supporting electrolyte; Glassy carbon (working), Pt wire (counter) and Ag/AgCl (reference); Scan rate: 100 mV s<sup>-1</sup>.*

**7. Langmuir-Blodgett film formation and characterizations.**

*a. Figure S4. Compression isotherm data of complex **2** and the ligand with their selected BAM micrographs.*

*b. Figure S5. The AFM images of monolayer films deposited on mica substrates at different surface pressures for complex **2** (a)-(f). Scan size of 5 μm for all images. Some dust particles were observed as pink-colored dots.*

*c. Figure S6. The IRRAS spectra of (a) complex **2** (b) C-H stretching region in comparison with KBr in bulk infrared spectra.*

**8. Electron Passivation Studies.**

*a. Figure S7. Cyclic voltammograms obtained for the passivation of gold electrode using different number of LB films of complex **1** and the ligand.*

*b. Figure S8. Cyclic voltammograms obtained for the passivation of 11-layer deposited gold electrodes of complexes **1**, **2** and the ligand before and after immersing in acid solution for 5 days.*

**9. Corrosion Analysis.**

*a. Figure S9. Images for acid corrosion using iron plates coated with complexes **1** and **2** (a)-(c) after one day and (d)-(f) after one week.*

*b. Figure S10. Optical micrograph images for blank and 11-layer LB film-coated iron plates (a)-(c) before corrosion, and (d)-(f) after acid corrosion.*

## 1. Experimental Section.

### a. Materials and methods.

Reagents were used without further purification as purchased from commercial sources.  $^1\text{H-NMR}$  spectra were recorded on a Varian 400 MHz instrument. Elemental analysis was measured by Midwest Microlab, Indianapolis, Indiana, USA using an Exeter CE440 CHN analyzer. ESI mass spectra were measured on a ZQ-Waters/Micromass high resolution mass spectrometer. The FT-IR spectra were obtained as KBr pellets from 4000 to 600  $\text{cm}^{-1}$  using 64 scans on a Tensor 27 FTIR-spectrophotometer. UV-visible spectra were obtained using a SHIMADZU UV-3600 spectrophotometer. Electrochemical experiments were performed using a BAS 50W voltammetric analyzer. For electrochemical experiments a standard three-electrode cell system was used with glassy carbon as the working electrode, Pt wire as the auxiliary electrode, and an Ag/AgCl reference electrode filled with 1 M KCl at room temperature. Tetrabutylammonium hexafluorophosphate ( $\text{TBAPF}_6$ ) was used as the supporting electrolyte and ferrocene was added to the solution as an internal redox standard for electrochemical experiments. For the passivation experiment, a Langmuir-Blodgett film deposited onto gold coated glass plate with *ca.* 0.7  $\text{cm}^2$  surface area was used as the working electrode. All the voltammograms were recorded at a scan rate of 100  $\text{mV s}^{-1}$ . A 0.20 mm thick iron foil (purity 99.5%) was used for corrosion experiments, as detailed later in this document.

## 2. Synthesis and characterizations.

### a. Synthesis of $[\text{Zn}^{\text{II}}(\text{L}^{\text{N}2\text{O}2})\text{H}_2\text{O}]$ (**2**).

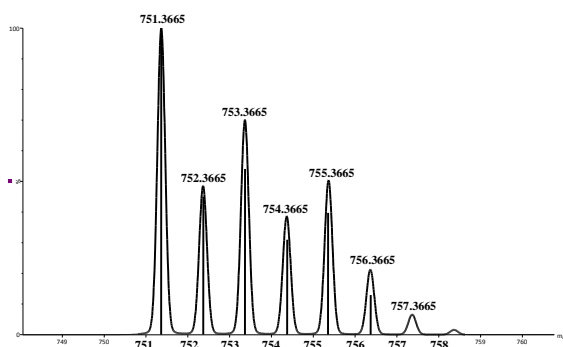
Complex **2** was synthesized by treating a methanol solution of  $[\text{H}_2\text{L}^{\text{N}2\text{O}2}]$  (0.1 g, 0.145 mmol) and  $\text{NaOCH}_3$  (0.016 g, 0.3 mmol) with zinc chloride under refluxing conditions. Orange needle-like crystals were isolated for  $[\text{Zn}^{\text{II}}(\text{L}^{\text{N}2\text{O}2})\text{CH}_3\text{OH}/\text{H}_2\text{O}]$  (**2**) from methanol: dichloromethane (3:1) solution.

*The crystalline product shows alternating molecules of  $[\text{Zn}^{\text{II}}(\text{L}^{\text{N}2\text{O}2})\text{H}_2\text{O}]$  and  $[\text{Zn}^{\text{II}}(\text{L}^{\text{N}2\text{O}2})\text{CH}_3\text{OH}]$  (See section 4, X-ray Determination). The former species is assumed prevalent in aqueous media.*

Yield: 80%. ESI ( $m/z$ ) in  $\text{CH}_3\text{OH}$  for  $[\text{Zn}^{\text{II}}(\text{L}^{\text{N}2\text{O}2}) + \text{H}^+]^+$  = 751.3667 (100%), with  $(\text{L}^{\text{N}2\text{O}2})^{-2} = \text{C}_{42}\text{H}_{58}\text{N}_2\text{O}_6$  in excellent agreement with the calculated value of  $m/z = 751.3665$  in agreement with 0.3 ppm difference. Anal. Calc. for  $[\text{C}_{42}\text{H}_{58}\text{ZnN}_2\text{O}_6 \cdot 0.5\text{H}_2\text{O} \cdot 0.5\text{CH}_3\text{OH}]$ : C, 65.67; H, 7.91; N, 3.60 %. Found: C, 65.51; H, 7.84; N, 3.71 %. IR (KBr,  $\text{cm}^{-1}$ ) 2869-2953 ( $\nu_{\text{C-H}}$ ), 1610 ( $\nu_{\text{C=C}}$ , aromatic), 1503 ( $\nu_{\text{C=C}}$ , aromatic) 1589 ( $\nu_{\text{C=N}}$ ), 1265 ( $\nu_{\text{C-O-C}}$ ), 1132 ( $\nu_{\text{C-O-C}}$ ).

## 3. Mass Spectrum for Complex 2.

### a. **Figure S1.** Experimental (bars) and simulated (line) isotopic distribution for the molecular ions of $[\text{Zn}^{\text{II}}(\text{L}^{\text{N}2\text{O}2}) + \text{H}^+]^+$ .



#### 4. X-ray structural determination for [Zn<sup>II</sup>(L<sup>N2O2</sup>)H<sub>2</sub>O/MeOH] (2).

Orange colored X-ray quality single crystals of complex **2** were obtained by slow evaporation of the complex dissolved in a 1:1 dichloromethane:methanol solvent mixture. A suitable crystal was selected and mounted on a mitogen loop, and diffraction data were collected on a Bruker X8 SMART APEX II CCD diffractometer using a monochromatic graphite-Mo K $\alpha$  radiation source (0.7107 Å) and SMART/SAINT52 software. The crystal was kept at 100.1 K during data collection and a total of 64892 reflections were collected, with 14123 unique reflections. Using the Olex2 structure solution suite,<sup>1</sup> the structure was solved with the ShelXS structure solution program using Direct Methods, and refined with the XL refinement package using Least Squares minimization.<sup>2</sup> Hydrogen atoms were placed in calculated positions. There are two independent penta-coordinated complexes, one with CH<sub>3</sub>OH and one with H<sub>2</sub>O in the axial positions respectively, and two methanol solvent molecules in the asymmetric unit. Selected crystallographic data is shown in **Table S1**. The complex shows a tau ( $\tau$ ) value of 0.13, which is consistent with a square pyramidal geometry.<sup>3</sup> The Zn–O and Zn–N bond lengths are consistent with reported literature values.<sup>4</sup>

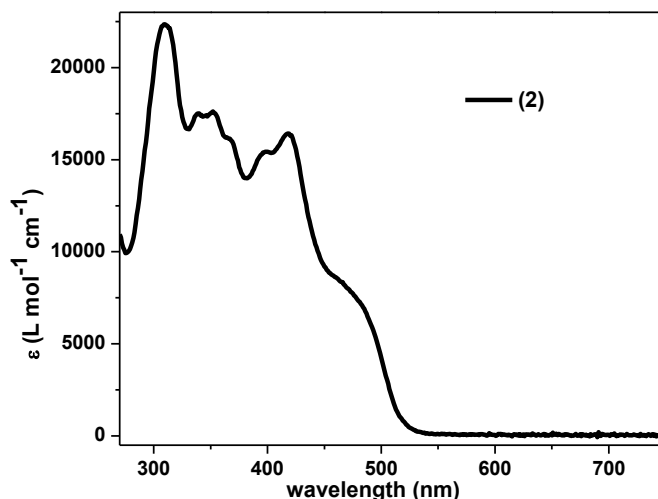
a. **Table S1.** Selected X-ray crystal data for complex **2**.

	(2)
Formula	C <sub>43</sub> H <sub>62</sub> N <sub>2</sub> O <sub>7</sub> Zn·C <sub>42</sub> H <sub>60</sub> N <sub>2</sub> O <sub>7</sub> Zn·2(CH <sub>4</sub> O)
M	1618.69
Temperature/K	100.1
Crystal system	Triclinic
Space group	<i>P</i> <sup>-</sup> 1
a/Å	14.3039 (16)
b/Å	17.603 (2)
c/Å	20.104 (2)
$\alpha$ /°	64.648 (6)
$\beta$ /°	74.715 (7)
$\gamma$ /°	86.046 (7)
Volume/Å <sup>3</sup>	4407.0 (9)
Z	2
D <sub>calc</sub> /g cm <sup>-3</sup>	1.220
$\mu$ /mm <sup>-1</sup>	0.610
R(F) (%)	8.90
Rw(F) (%)	22.8

$$^a R(F) = \sum \left| |F_o| - |F_c| \right| / \sum |F_o|; \quad R_w(F) = [\sum w(F_o^2 - F_c^2)^2 / \sum w(F_o^2)]^{1/2} \text{ for } I > 2\sigma(I)$$

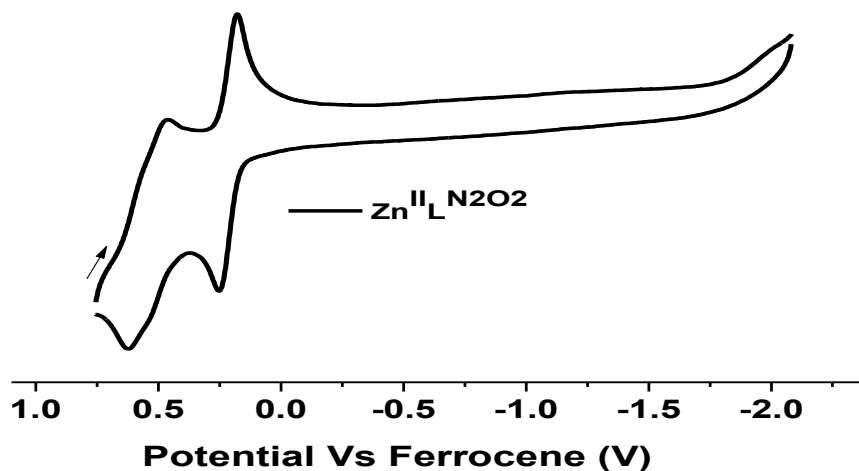
## 5. Electronic Spectrum for Complex 2.

a. **Figure S2.** UV-visible spectrum of **2** in  $1 \times 10^{-5}$  M dichloromethane.



## 6. Electrochemical Data for the Complex 2.

a. **Figure S3.** Cyclic voltammogram of **2** in dichloromethane. Conditions: 0.1 M TBAPF<sub>6</sub> as supporting electrolyte; Glassy carbon (working), Pt wire (counter) and Ag/AgCl (reference); Scan rate: 100  $\text{mV s}^{-1}$ .

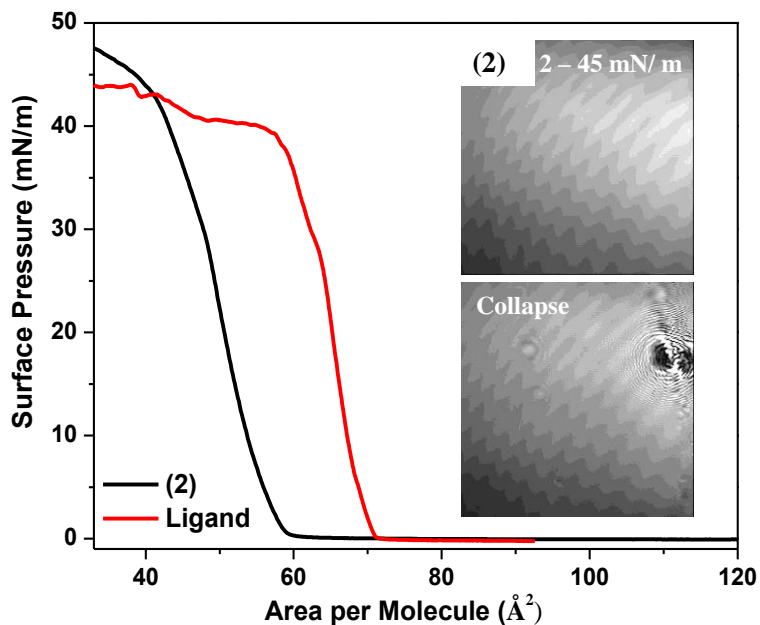


## 7. Langmuir-Blodgett film formation and characterizations.

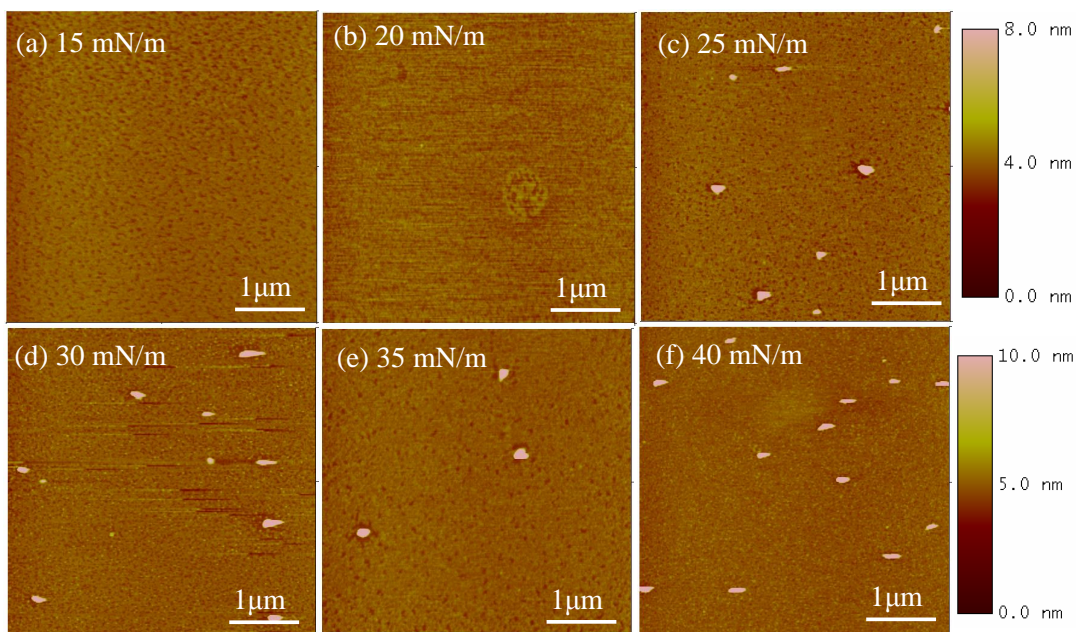
The compression isotherm for complex **2** was measured using an automated KSV 2000 mini trough at 23 °C with a 10 mm/min compression rate. Barnstead NANOpure water with  $18.2 \text{ M}\Omega \text{ cm}^{-1}$  resistivity was used as the subphase. A 50  $\mu\text{l}$  of 1.0 mg/ml chloroform solution of the complex was spread on the subphase and allowed 20 min time for phase equilibrium and solvent evaporation before compression. For the IRRAS and corrosion measurements the layers were deposited at a transfer surface pressure of 30 mN/m for the ligand and 33 mN/m for complexes **1** and **2**. The transfer rate was 4 mm/min for the

ligand, complexes **1** and **2**. The field view was 800 x 600 microns and the lateral resolution was about 2  $\mu\text{m}$ . The deposition transfer ratios were close to one as indicative of near complete transfer onto the surface and the y-type dipping method was used for all the depositions.

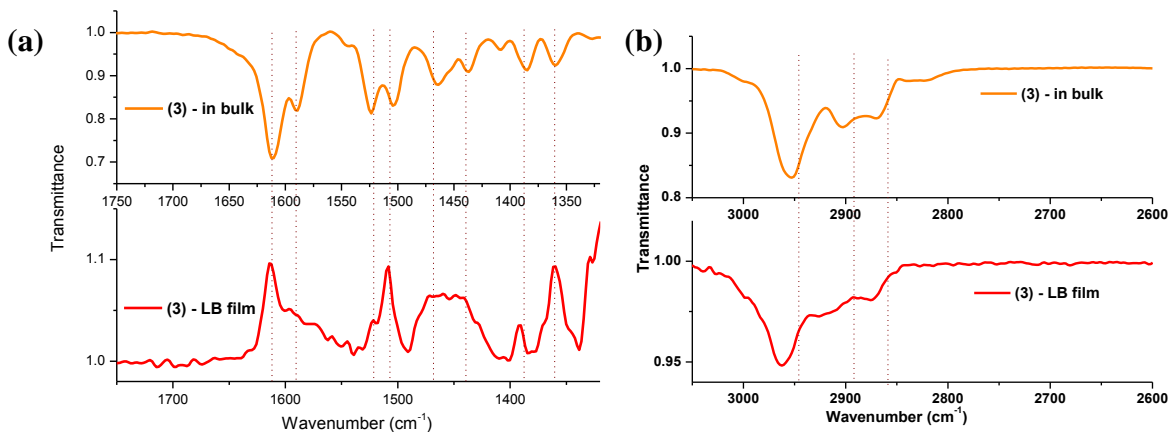
a. **Figure S4.** Compression isotherm data of complex **2** and the ligand with their selected BAM micrographs.



b. **Figure S5.** The AFM images of monolayer films deposited on mica substrates at different surface pressures for complex **2** (a)-(f). Scan size of 5  $\mu\text{m}$  for all images. Some dust particles were observed as pink-colored dots.

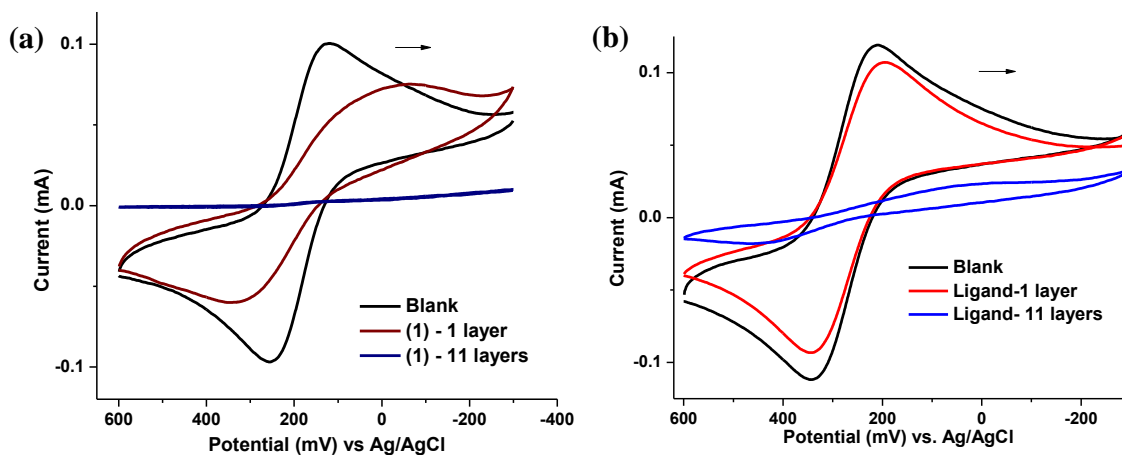


c. **Figure S6.** The IRRAS spectra of (a) complex **2** (b) C-H stretching region in comparison with KBr in bulk infrared spectra.

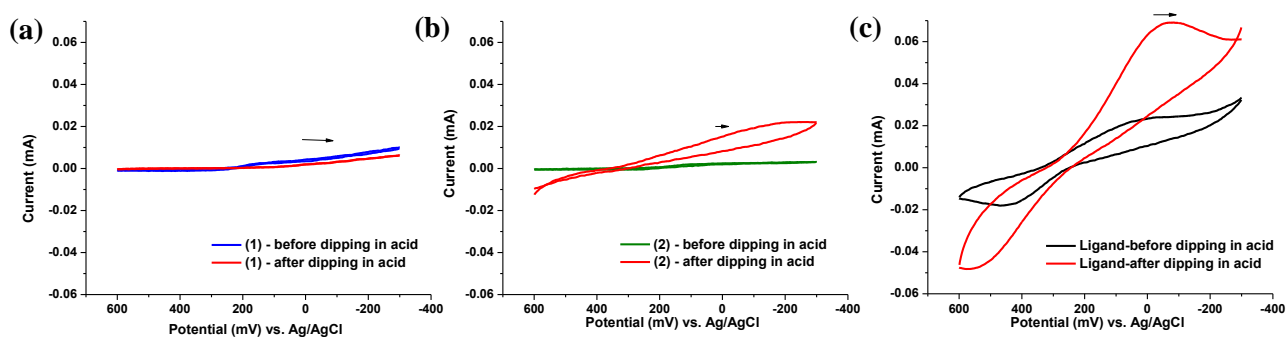


## 8. Electron Passivation Studies.

a. **Figure S7.** Cyclic voltammograms obtained for the passivation of gold electrode using different number of LB films of complex **1** and the ligand. Scan rate: 100 mV s<sup>-1</sup>.



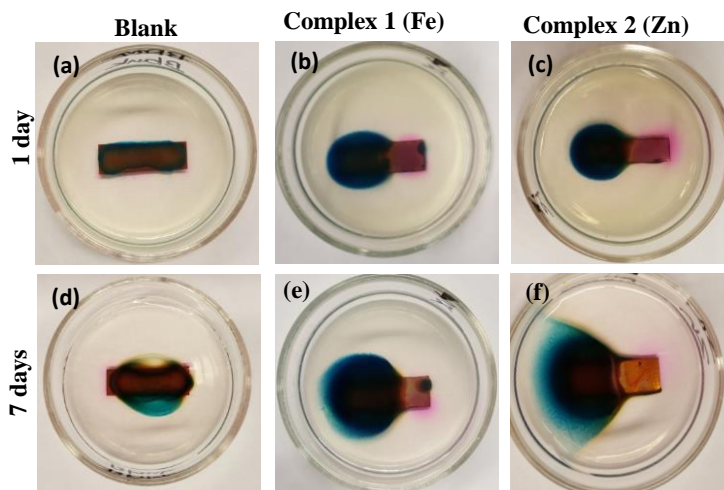
b. **Figure S8.** Cyclic voltammograms obtained for the passivation of 11-layer deposited gold electrodes of complexes **1**, **2** and the ligand before and after immersing in acid solution for 5 days.



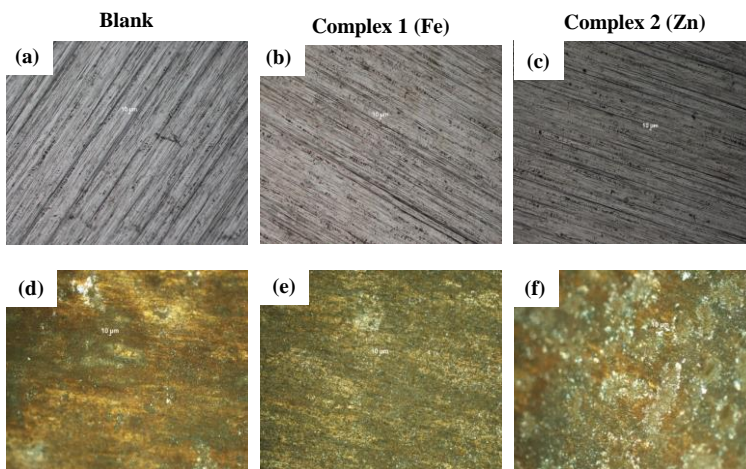
## 9. Corrosion Analysis.

An iron foil of 0.20 mm thickness (purity 99.5+ %) was used to prepare the specimens. Prior to each experiment, the iron foil was cleaned using alumina powder (0.05 micron), then rinsed with ethanol and nanopure water, and was air dried. For the weight loss measurements, iron plates in triplicate were immersed in 10 mL of corrosive solutions at room temperature.

a. **Figure S9.** Images for acid corrosion using iron plates coated with complexes **1** and **2** (a)-(c) after one day and (d)-(f) after one week.



b. **Figure S10.** Optical micrograph images for blank and 11-layer LB film-coated iron plates (a)-(c) before corrosion, and (d)-(f) after acid corrosion.



[1] O. V. Dolomanov, L. J. Bourhis, R. J. Gildea, J. A. K. Howard, and H. J. Puschmann, *Appl. Cryst.*, 2009, **42**, 339.

[2] G. M. Sheldrick, *Acta Cryst.*, 2008, **A64**, 112.

[3] A. W. Addison, T. N. Rao, J. Reedijk, J. van Rijn, and G. C. Verschoor, *Dalton Trans.* 1984, **7**, 1349.

[4] O. Rotthaus, O. Jarjays, F. Thomas, C. Philouze, E. Saint-Aman, and J. Pierre, *Dalton Trans.* 2007, 889.